



HAL
open science

Quantitative assessment of coagulation of atmospheric particles onto airborne birch pollen grains

M. Choël, Anastasia Ivanovsky, Antoine Roose, Mona Hamzé, Anne-Marie Blanchenet, Nicolas Visez

► **To cite this version:**

M. Choël, Anastasia Ivanovsky, Antoine Roose, Mona Hamzé, Anne-Marie Blanchenet, et al.. Quantitative assessment of coagulation of atmospheric particles onto airborne birch pollen grains. *Journal of Aerosol Science*, 2021, 161, pp.105944. 10.1016/j.jaerosci.2021.105944 . hal-03506095

HAL Id: hal-03506095

<https://hal.science/hal-03506095>

Submitted on 5 Jan 2023

HAL is a multi-disciplinary open access archive for the deposit and dissemination of scientific research documents, whether they are published or not. The documents may come from teaching and research institutions in France or abroad, or from public or private research centers.

L'archive ouverte pluridisciplinaire **HAL**, est destinée au dépôt et à la diffusion de documents scientifiques de niveau recherche, publiés ou non, émanant des établissements d'enseignement et de recherche français ou étrangers, des laboratoires publics ou privés.

1 Quantitative Assessment of Coagulation of Atmospheric

2 Particles onto Airborne Birch Pollen Grains

3 Marie Choël¹, Anastasia Ivanovsky¹, Antoine Roose¹, Mona Hamzé^{1,2}, Anne-Marie
4 Blanchenet³, Nicolas Visez^{*1}

5 1. Univ. Lille, CNRS, UMR 8516 - LASIRE - Laboratoire de Spectroscopie pour les
6 Interactions, la Réactivité et l'Environnement, F-59000 Lille, France

7 2. Univ. Lille, CNRS, UMR 8522 - PC2A - Physicochimie des Processus de
8 Combustion et de l'Atmosphère, F-59000 Lille, France

9 3. Univ. Lille, CNRS, UMR 8207 - UMET - Unité Matériaux et Transformations,
10 Lille, F-59000, France

11
12 * **Corresponding author:** Nicolas Visez (nicolas.visez@univ-lille.fr)

13 Batiment C5 – LASIRE

14 Université de Lille - Cité Scientifique

15 59655 Villeneuve d'Ascq

16 FRANCE

17
18 **Keywords:** Environmental pollution, particulate matter, atmospheric pollen
19 sampling, pollen allergy.

20 **ABSTRACT**

21 The coagulation of airborne particles on the surface of allergenic pollen grains is
22 poorly described in the literature. However, particles deposited on the surface of
23 pollen grains could have an effect on allergy and its symptoms. Observations of pollen
24 surface alterations reported in the literature are either qualitative or are tainted by
25 sampling artifacts that overestimate surface particulate pollution. Birch pollen grains
26 (BPGs) were sampled in the atmosphere during pollination to quantitatively assess
27 the extent of particulate deposition on allergenic pollen surfaces. Airborne PGs were
28 collected with a cascade impactor ensuring no sampling artefact unlike pollen
29 samplers usually used in this type of study. Counting, sizing and elemental analysis of
30 particles adhering on pollen surfaces were performed by SEM/EDX. 68% of PGs did
31 not carry any particle on their visible surface while the remaining 32% had between 1
32 to 16 particles on their surface. On average, polluted BPGs carried 2 ± 1 particles,
33 representing an average surface coverage of 0.95%. We hypothesized that the main
34 coagulation process was particle deposition by gravitational settling. Collision
35 velocity calculations indicate that coagulation due to gravitational settling is
36 prevalent under typical pollination atmospheric conditions. However, the effects of
37 electric charges carried by pollen are largely unknown and may significantly alter
38 coagulation rates. The presence of particle-polluted allergenic pollens appears to be
39 common in the urban atmosphere, even under low air pollution conditions. The
40 impact of chemical pollution of BPGs due to the presence of particulate matter
41 (including soot particles) remains relatively unknown, both on the allergy and on the
42 reproductive capacity of the tree.

43

44

45 **1.INTRODUCTION**

46 Birch pollen grains (BPGs) cause allergic reactions in more than 100 million people
47 worldwide (Lavaud et al., 2013). An increasing trend in atmospheric BPG
48 concentrations has been observed in several countries in relation to the relentless rise
49 of carbon dioxide and the effects of climate change (Besancenot et al., 2019; Darbah
50 et al., 2008; Frei, 1998; Hoebeke et al., 2017; Ziska et al., 2019). In addition, air
51 pollution can aggravate allergy symptoms (Robichaud, 2021; Schiavoni et al., 2017).
52 The allergic patient indeed never breathes BPGs alone; airborne BPGs are suspended
53 in the urban atmosphere consisting of gaseous pollutants (NO₂, O₃, Volatile Organic
54 Compounds), coarse, fine and ultrafine particles and other bioaerosols (spores and
55 other potentially allergenic pollens). Taken separately, each of the constituents of the
56 urban atmosphere can have aggravating effects on allergy but physical-chemical
57 interactions also exist between gaseous and particulate atmospheric compounds.
58 Alterations of BPGs due to atmospheric biochemical reactions with ozone or nitrogen
59 dioxide have been highlighted (Sénéchal et al., 2015). Gaseous air pollutants modify
60 the lipid and protein fraction of BPGs (Farah et al., 2021; Pereira et al., 2021; Visez et
61 al., 2020). Not only pollen grains (PGs) can be modified by air pollution, but there are
62 clear qualitative evidences that allergenic PGs can also act as carriers of pollutants,
63 both adsorbed gases and coagulated particles (Okuyama et al., 2007; Zhu et al.,
64 2018).

65 Particulate pollution of the surface of allergenic PGs is, unlike pollen-gas interactions,
66 poorly assessed in the literature (Visez et al., 2020). Most of the observations of
67 particles on the surface of PGs are qualitative reports that do not estimate the extent
68 of the pollution of the surface of PGs by extrapollinic atmospheric particles. The
69 available quantitative studies report particularly high pollution of PG surfaces. For

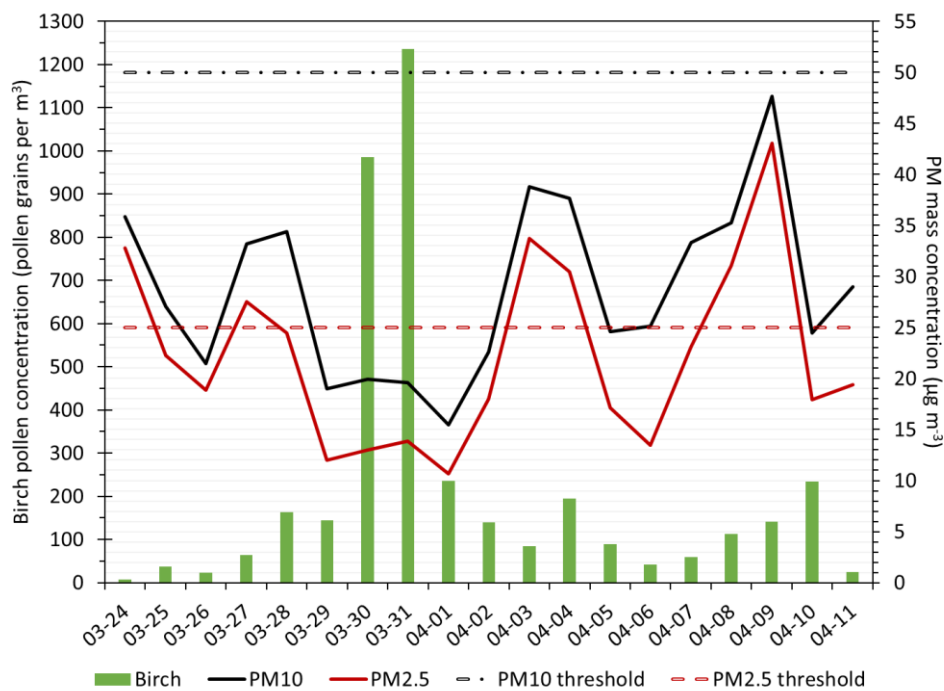
70 instance, Ribeiro et al. (2015) reported an average number of particles adhering to
71 the pollen surface of 16 ± 12 (average \pm standard deviation), 39 ± 32 and 4 ± 4
72 particles per PG for *Acer*, *Pinus* and *Platanus* pollen, respectively (Ribeiro et al.,
73 2015). This study was conducted using a Hirst volumetric spore trap which is the
74 most common method of sampling pollen on a moving slide, originally developed to
75 count ambient pollen (Mullins & Emberlin, 1997). However, the use of a Hirst-type
76 pollen sampler induces a sampling artifact with a significant overestimation of
77 particle adhesion on PGs (Choël et al., 2020). In addition, to our knowledge, there are
78 no quantitative data on the specific pollution of the surface of BPGs by atmospheric
79 particulate matter (APM); only one study reported a high degree of particle
80 agglomeration onto BPGs collected from two highly polluted urban areas (Behrendt
81 et al., 1991).

82 Being able to sample windborne PGs while preserving their initial state is crucial to
83 study how PM alters the physical, chemical and biological properties of PGs. PM
84 pollution of PGs can only be adequately assessed if particle size-selective
85 classification is employed when sampling airborne pollen. In such way, PGs can be
86 efficiently trapped in a specific sampling stage (for coarse particles) different from
87 smaller ambient particles (Levetin, 2004). Moreover, the sampling efficiency of
88 airborne PGs is improved by the use of low nozzle velocity devices, such as impactors,
89 compared to active sampling pollen trap, such as Hirst-type samplers (Choël et al.,
90 2020; Ribeiro et al., 2015; Wittmaack et al., 2005). In addition, the sampling
91 duration should be short enough (~a few hours) to avoid the pile-up of particles,
92 especially in highly polluted environments (Wittmaack et al., 2005). The objective of
93 this work is to document and reliably assess the size range, particle types and
94 frequency of occurrence of particles adhered to airborne BPGs sampled under fairly

95 clean air conditions. Sampling of airborne PGs was carried out for the first time in the
96 literature with a cascade impactor ensuring collection of PGs without piling up of fine
97 particles on their surface in the collector during sampling (i.e., free from sampling
98 artifact).

99 2. MATERIALS AND METHODS

100 Pollen sampling was carried out daily from 30 March to 7 April 2017 (start and end
101 time: 10:00 am) on the roof of a building of Lille University campus (Lat. 50° 36' 29"
102 N, Long. 3° 8' 25" E, Altitude 20 m a.s.l.) (Supplementary Figure S0) when weekly
103 cumulative birch pollen concentrations peaked at 3022 grains·m⁻³ according to the
104 French monitoring network (RNSA) in Lille metropolitan area (Figure 1). On 30 and
105 31 March 2017, daily birch pollen concentrations peaked at 986 and 1236 BPGs per
106 m³, respectively. Meteorological parameters were recorded by a weather station
107 (Davis Vantage Pro) installed at the sampling site (Supplementary Figure S1).



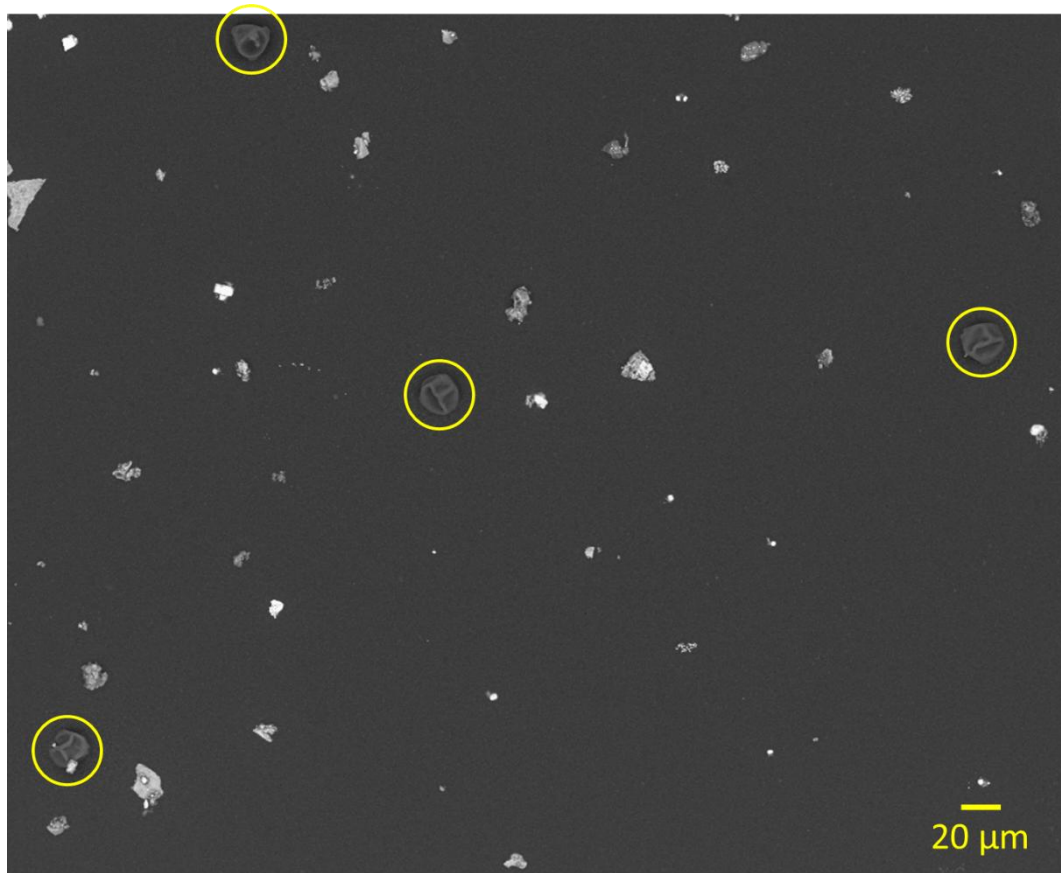
108

109 Figure 1. Daily concentrations of birch pollen grains in Lille metropolitan area (green bars) and
110 ambient PM₁₀ and PM_{2.5} mass concentrations during pollen sampling (respectively black and red

111 curves). Threshold values recommended by the World Health Organization were reported in black
112 dotted line for PM₁₀ (50 µg·m⁻³) and in red dotted line for PM_{2.5} (25 µg·m⁻³).

113 No rain event occurred during the study period. Birch dehiscence was triggered by a
114 temperature rise to 16°C combined with a drop of relative humidity on 30 March. The
115 weekly average temperature, relative humidity, and wind speed were 11.9 ± 2.2 °C,
116 76.7 ± 5.1 % RH, 1.4 ± 0.5 m·s⁻¹, respectively. Ambient PM₁₀ and PM_{2.5} concentrations
117 were 26.3 ± 8.3 µg·m⁻³ and 19.3 ± 8.2 µg·m⁻³, respectively at the closest air quality
118 monitoring station located 4 km away from the pollen sampling site (public data
119 provided by ATMO Hauts-de-France). During the study period, PM₁₀ concentrations
120 never exceeded the WHO recommended threshold value, i.e. 50 µg·m⁻³ (24-hour
121 mean). In contrast, PM_{2.5} concentrations were over the WHO guideline of 25 µg·m⁻³
122 (24-hour mean) on 3 and 4 April 2017 (Figure 1). Airborne PGs were trapped on the
123 first stage PM_{>10} µm of a 3-stage cascade impactor (PM₁₀ impactor, Dekati Ltd.), i.e.
124 impaction stage with particle size cut-off diameter of 10 µm at 50% collection
125 efficiency valid for spherical particles with a mass density of 1 g·cm⁻³. The impactor
126 was mounted on the top of a 4-meter-high mast (Supplementary Figure S2). Airborne
127 PGs were impacted directly on a conductive carbon tape for electron microscopic
128 examination. Bounce-off and re-entrainment of deposited PGs from the impaction
129 surfaces can be minimized by using adhesive collection substrates (Wittmaack et al.,
130 2005).

131 A number of 236 PGs were observed directly on the collection substrate without
132 metal coating using a low-vacuum SEM (JEOL JSM 7800F LV) operated at a working
133 pressure of 100 Pa in the specimen chamber. Visual detection of BPGs was carried
134 out by low magnification SEM inspection of the whole area of daily collection
135 substrates (circular surface with a diameter of 25 mm) (Figure 2).



136

137 Figure 2. Example of SEM image of birch pollen grains (circled) and atmospheric particulate matter
138 deposited on PM_{>10} µm impaction stage. The pollen grain on the bottom left carries atmospheric
139 particles.

140 As the impaction surface was static in the case of our PM₁₀ impactor, large particles
141 might pile up on top of pollen grains during sampling. The probability of having a
142 particle pile-up increases with the sampling duration. A typical view of the substrate
143 loading in the case of our daily sampling is presented in Figure 2. As can be seen,
144 after 24-hour sampling on PM_{>10} impaction stage, the particulate load on the
145 collection substrate was low, with BPGs well-separated from the other collected
146 particles, ensuring a minimized sampling artifact (Choël et al. 2020).

147 BPGs were detected by using backscattered electron (BSE) imaging. Because BSE
148 yield depends on the atomic number of the atoms causing the backscattering, BSE
149 images are sensitive to the elemental make-up of particles. BPGs are predominantly

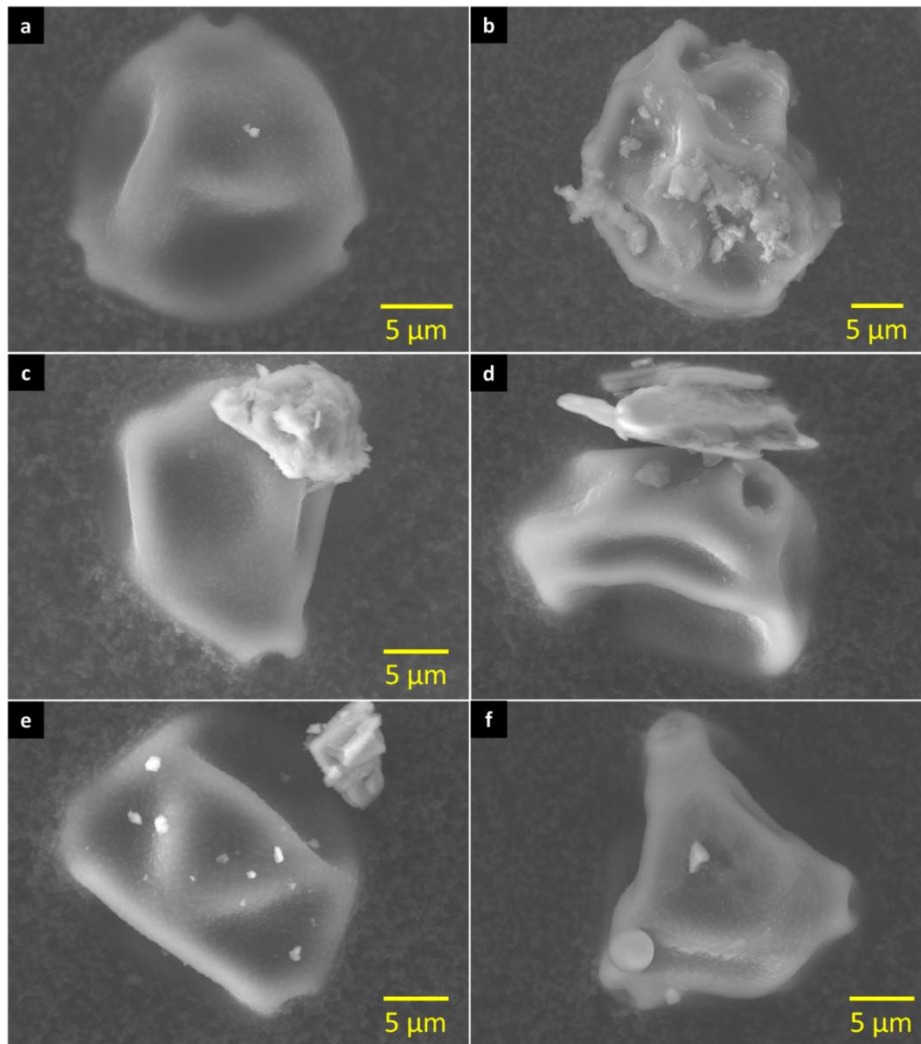
150 made up of light elements such as the carbon substrate. As a result, BPGs and the
151 substrate appear with similar grey levels. To confirm the presence of a BPG and to
152 examine particulate adhesion, each BPG was magnified and secondary electron (SE)
153 images sensitive to topography were taken. Counting and sizing of particles adhering
154 to pollen surfaces were determined from BSE images using FIJI/ImageJ software. X-
155 ray elemental analysis of particles attached to PGs was carried out with an energy-
156 dispersive X-ray (EDX) detector (SDD 80 mm², Oxford Instruments Inc.) at an
157 accelerating voltage of 15 kV. Note that BPGs appear deflated as a result of shrinkage
158 due to low-vacuum which enables EDX analysis of micrometer-sized particles down
159 to 0.2 μm (Choël et al., 2010).

160 **3.RESULTS**

161 A total of 236 BPGs were individually imaged by low-vacuum SEM/EDX and a total
162 of 205 particles were observed on birch pollen surfaces. 68% of PGs did not carry any
163 particle on their visible surface. The remaining 32% of PGs had between 1 and 16
164 particles adhered to their surface. On average, polluted PGs had 2 ± 1 particles on
165 their surface. Sampling artifact was assessed to 2.2 ± 2.4 particles per PG with a
166 conventional Hirst-type sampler under similar PM₁₀ and PM_{2.5} concentrations
167 (Choël et al., 2020). The low number of particles observed on birch pollen (2 ± 1
168 particles per BPG) confirms the need to use an impactor because the sampling
169 artifact of an HTS is of the same order of magnitude.

170 Particles deposited on BPGs had an average diameter of $1.5 \pm 2.0 \mu\text{m}$ (average \pm
171 standard deviation) and ranged in size from 0.2 to 11.8 μm . Polluted PGs had
172 particles covering an average of 0.95% of their surface. Particles lying on the
173 substrate had an average diameter of $5.6 \pm 4.0 \mu\text{m}$ with sizes varying between 0.3 and
174 21.9 μm (total number of particles observed on the substrate=309). Both the average

175 diameter and the size range were larger on the collection substrate compared to PG
176 surface, indicating a good size differentiation between PGs and fine particles in
177 suspension using PM_{>10} impaction sampling device. Two other types of PGs, namely
178 willow (*Salix L.*) and hornbeam (*Carpinus betulus*), were also observed with particles
179 adhering on their surface (Supplementary figures S3 and S4).

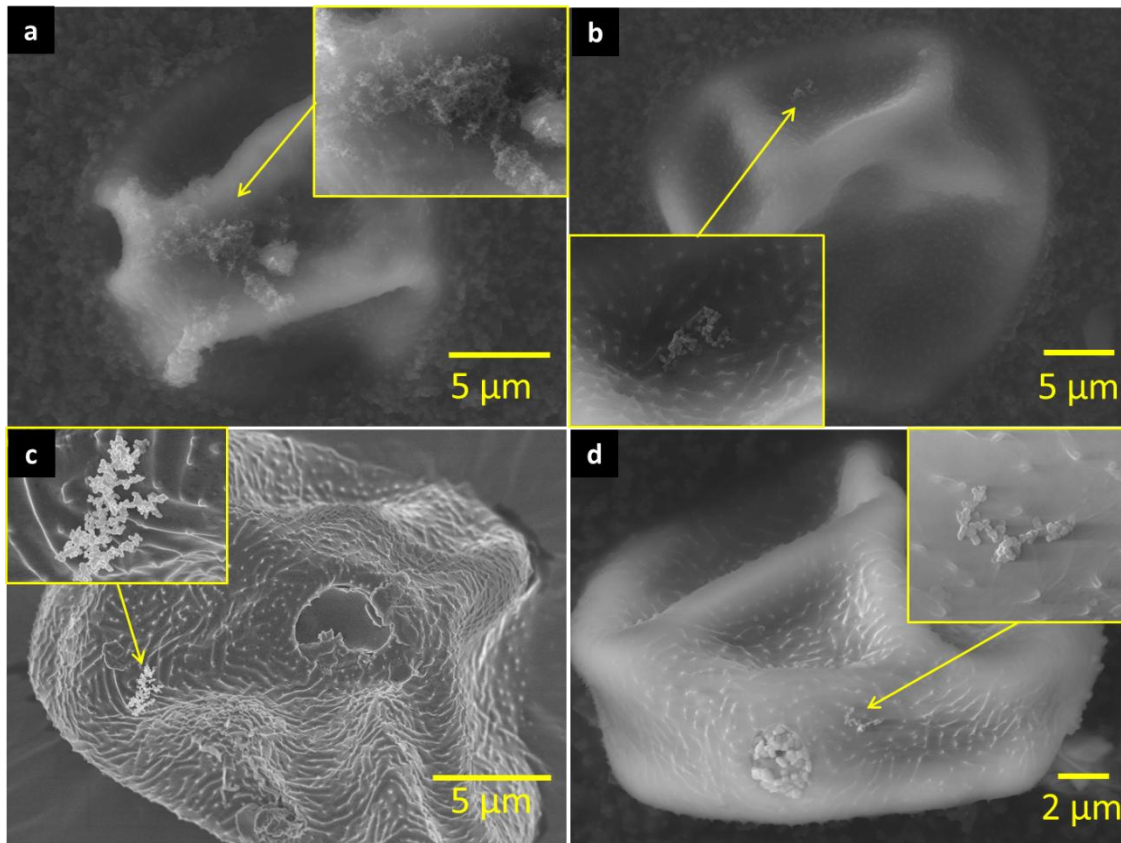


180

181 Figure 3. SEM images of polluted birch pollen grains carrying: (a) 1 µm-sized calcium silicate particle;
182 (b) aluminosilicate particles; (c) a large soil dust particle (plagioclase Al-Si-Ca-Fe-rich); (d) a large
183 phyllosilicate particle, (e) one supermicron and a dozen submicron dolomite particles; (f) a spherical
184 coal fly ash particle (O-Al-Si-rich diam 3.5 µm), a calcite particle (up) and a gypsum particle (down).

185 The nature of particles adhered to BPGs were as follow (Figure 3 and Figure 4): soil
186 dust (calcite, quartz, orthoclase (potassium feldspath), plagioclase, olivine, clay

187 minerals (illite, smectite, mica)), sea-salts, metal-rich (Fe-rich, Cu-rich, Ni-rich, Zn-
188 rich, Ba-rich) particles, small and large soot aggregates consisting of clusters of
189 nanospheres with a diameter of 40 to 90 nm.



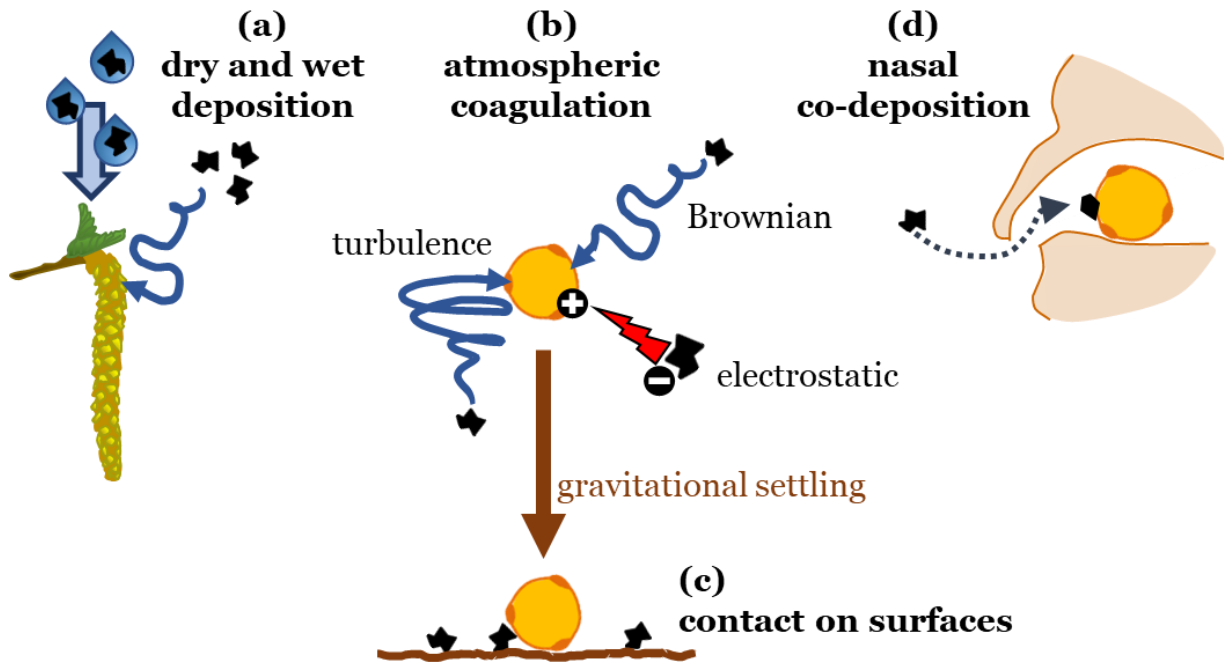
190

191 Figure 4. SEM images of polluted birch pollen grains: (a) covered with a large chain-like soot aggregate
192 of nanospheres (diameter 40-50 nm); (b-c) carrying a micrometer-sized chain-like soot aggregate of
193 nanospheres (diameter 80-90 nm); (d) with a soot aggregate (area equivalent diameter 1.1 μm) and
194 recrystallized sea-salts.

195 **4.DISCUSSION**

196 Our atmospheric samples collected under conditions of moderate particulate air
197 pollution reveals that pollution of the surface of pollen grains (PGs) by atmospheric
198 particles is a common phenomenon: out of a total of 236 birch pollen grains (BPGs)
199 examined, 32% of BPGs carried an average of 2 ± 1 particles (205 particles deposited
200 on 75 BPGs). On a global average during our sampling, BPGs carried 0.86 particles
201 (205 particles observed particles for 236 BPGs). The fraction of the pollen surface

202 covered by particles is however very low, less than 1%, which contrasts with the
203 higher fractions previously reported in the literature (Behrendt et al., 1991; Ribeiro et
204 al., 2015). For example, the area covered by particles on pine and maple pollen
205 collected from the atmosphere with a Hirst trap was 5.7% and 7.5%, respectively
206 (Ribeiro et al., 2015). A very high degree of agglomeration was also observed for BPG
207 collected with a high volume sampler in highly polluted urban areas (Behrendt et al.,
208 1991). We assume that the high degrees of agglomeration presented in these previous
209 works may be subject to a sampling artefact involving an overestimation of the
210 number of particles per PG. Hirst-type samplers are not suitable for the assessment
211 of particulate pollution on the surface of PGs due to a too high impaction velocity
212 which does not allow the discrimination of pollen and PM₁₀ during sampling (Choël
213 et al., 2020). The use of a PM₁₀ impactor avoids this sampling artefact and explains,
214 at least in part, the lower particulate pollution rate obtained in this study (Choël et
215 al., 2020). Another explanation is that the air quality was relatively good in our study
216 (PM₁₀ = 26.3 ± 8.3 µg·m⁻³), which reduces the probability of coagulation of
217 atmospheric particles on the surface of PGs. One of the limitations of our study is the
218 low number of PGs observed. Manual grain-by-grain observation by electron
219 microscopy is indeed time-consuming and unsuitable for samples of several thousand
220 grains but it is the only way to reliably assess the presence of particles on PGs. In
221 addition, some particles are difficult to identify, in particular due to the presence of
222 sub-pollen particles on the surface of BPGs (Ruggiero & Bedini, 2018, 2020). It
223 should also be remembered that SEM analysis only allows to observe the visible
224 pollen surface; particles stuck to the pollen surface on the side of the collection
225 substrate (hidden surface) are obviously not observable.



226

227 Figure 5. Proposed mechanisms for coagulation of atmospheric particles on the surface of pollen
 228 grains. The yellow balls represent birch pollen grains. The black pictograms symbolize atmospheric
 229 particles.

230 The pollution rate of BPGs obtained in our sampling can be explained by several
 231 mechanisms of APM deposition (Figure 5) without the possibility to assign their
 232 respective relative contributions: dry and wet deposition on catkins before pollination
 233 (a), coagulation in the atmosphere (b), contact after deposition on a surface polluted
 234 by particles followed by resuspension of the PG (c). Particulate pollution on catkins
 235 and resuspension of PGs need to be specifically studied as these mechanisms are
 236 poorly documented (Visez et al., 2020).

237 On the other hand, it is possible to estimate by calculation the contribution of
 238 coagulation of particles with PGs in the atmosphere (Figure 5 (b)); particles
 239 coagulation is described by the rate of collision J_{12} (particles.s⁻¹) between two
 240 populations of particles at concentrations N_1 and N_2 (equation 1, Table) (Seinfeld &
 241 Pandis, 2016). Equations 1 to 4 (Table) describe respectively Brownian coagulation,
 242 gravitational coagulation and coagulation in turbulent flow (García-Nieto, 2006;

243 Seinfeld & Pandis, 2016). The coagulation rates could also be influenced by the
 244 electrical charges of particles (Harrison & Carslaw, 2003) ; however, the lack of data
 245 on the distribution of electrical charges in our sampling conditions does not allow to
 246 estimate this specific contribution (enhancement, no effect or reduction) on the
 247 deposition rates of APM on BPGs.

248 Table 1. Equations for the rate of collision J_{12} between particles 1 and 2 (eq. 1) and coagulation rate
 249 coefficients K_{12} for Brownian coagulation (eq. 2), gravitational coagulation (eq. 3) and coagulation in
 250 turbulent flow (eq. 4) (García-Nieto, 2006; Seinfeld & Pandis, 2016).

Equation 1		N particle concentration (#.m ⁻³)
Rate of collision	$J_{12} = K_{12}N_1N_2$	K_{12} coagulation rate coefficients
Equation 2		k Boltzmann constant; μ viscosity of air (20°C, 1.825×10 ⁻⁵ kg·m ⁻¹ ·s ⁻¹); T temperature (K); D_p diameter of particles (m); C_c Cunningham correction factor
Brownian coagulation	$K_{12}^{BG} = \frac{2kT}{3\mu} (D_{P1} + D_{P2}) \left(\frac{C_{C1}}{D_{P1}} + \frac{C_{C2}}{D_{P2}} \right)$	
Equation 3		ϑ_t terminal settling velocity (BPGs = 0.012 m·s ⁻¹ ((Sofiev et al., 2006))); $E(D_{P1}, D_{P2})$ collision efficiency (=1 in this work)
Gravitational coagulation	$K_{12}^{GC} = \frac{\pi}{4} (D_{P1} + D_{P2})^2 (\vartheta_{t1} - \vartheta_{t2}) E(D_{P1}, D_{P2})$	
Equation 4		ε_k rate of dissipation of kinetic energy per unit mass (10 s ⁻¹); ν kinematic viscosity of fluid = (15.06×10 ⁻⁶ m ² ·s)
Coagulation in turbulent flow	$K_{12}^{TF} = \left(\frac{\pi^2 \varepsilon_k}{120\nu} \right)^{1/2} (D_{P1} + D_{P2})^3$	

251
 252 Calculations of K_{12} for the three types of coagulation described in Table were
 253 performed for a particle deposition on BPG (21 μ m in diameter) from a monomodal
 254 population of 2 μ m diameter particles at a concentration of 5 particules·cm⁻³,

255 considering a terminal settling velocity of $100 \text{ cm}\cdot\text{h}^{-1}$ for particles ($1.2 \text{ cm}\cdot\text{s}^{-1}$ for BPG)
256 and no rebounds after collision. This computational estimate shows that K_{12} is of the
257 same order of magnitude for gravitational coagulation ($K_{12}^{GC} \approx 4.8 \times 10^{-12} \text{ m}^6\cdot\text{s}^{-1}$) as for
258 turbulence ($K_{12}^{TF} \approx 1.6 \times 10^{-12} \text{ m}^6\cdot\text{s}^{-1}$) while K_{12}^{BG} related to Brownian motion is largely
259 negligible ($K_{12}^{BG} \approx 2 \times 10^{-15} \text{ m}^6\cdot\text{s}^{-1}$). Equation 3 tends to predict very high coagulation
260 with the finer particles, as the difference in settling velocity is greater and the
261 concentrations of the fine particles are several thousands to tens of thousands of
262 particles per cm^3 . However, the efficiency of collision E_{12} , which depends on the size
263 of the particles involved, decreases sharply as the diameter of particle 2 tends
264 towards zero (Seinfeld & Pandis, 2016). This prediction is consistent with our
265 observations where relatively few very fine particles ($< 500 \text{ nm}$) were detected on the
266 surface of BPGs.

267 Under typical pollination weather conditions (absence of turbulence, calm weather
268 and low wind), and without taking into account electrostatic interactions between
269 particles, the main coagulation process would be the deposition of particles by
270 gravitational settling. By assuming a concentration of $2\text{-}\mu\text{m}$ -sized particles N_2 in the
271 order of $5 \text{ particles}\cdot\text{cm}^{-3}$ and a gravitational settling time of one hour (drop of 43 m),
272 we calculate 0.09 particles deposited per PG ($J_{12} = 2.4 \times 10^{-5} \text{ particles}\cdot\text{s}^{-1}$). For pollen
273 transported over long distances, while some PGs have been observed at considerable
274 altitudes of 2 km (Damialis et al., 2017), it is conceivable that gravitational settling
275 alone explains the levels of particulate contamination of PGs observed in our samples
276 (on average 0.86 particles per BPG). If the hypothesis of coagulation primarily by
277 gravitational settling is correct, then the presence of particles on the surface of BPGs
278 could be a marker of atmospheric transport of pollen over long distances.

279 Our coagulation calculations shed interesting light on the hypothesis of increased
280 COVID-19 propagation by virus transport on the surface of PGs (Damialis et al., 2021;
281 Dbouk & Drikakis, 2021). The thousands of droplets emitted by exhalation, and
282 potentially infected by a virus, are in the micrometre to 100 μm range, with a
283 maximum around 50 to 150 μm (Xie et al., 2009). Our estimates show that the
284 encounter between a PG and a coarse particle of about 100 μm will be very unlikely
285 for contact times of a few minutes. For fine particles (2 μm) exhaled at a
286 concentration of 150,000 particles $\cdot\text{m}^{-3}$ in contact with a high concentration of BPGs
287 (1,000 BPGs $\cdot\text{m}^{-3}$), the calculated deposition rate of 2- μm -sized particles on pollen is
288 0.06 particles per day (Shao et al., 2021). In light of these estimates of the
289 coagulation rate and the low number of particles observed on the surface of pollen in
290 our atmospheric samples, the transport by a PG of a virus expectorated by a human
291 being is most likely a rare event. If pollen is involved in the aggravation of COVID
292 infection (Gilles et al., 2021; Khaiwal et al., 2021), we suggest that co-exposure to
293 expectorated droplets and PGs is more likely involved than virus adhesion to the
294 pollen surface. More precise modelling work is needed; our estimates by calculating
295 the coagulation rate of particles on pollen are only intended to give orders of
296 magnitude of the coagulation phenomena involved.

297 The observation of several PGs with soot suggests that combustion-emitted particles
298 may have a particular affinity with pollen. It has been suggested that electrostatic
299 interactions may promote affinity between combustion particles and bioaerosols
300 (Roos & Dutertre-Laduree, 1990). However, the number of BPGs with soot is too
301 small to provide a reliable estimate of occurrence of soot sticking on BPGs in the
302 urban atmosphere. Furthermore, the sampling was conducted on the roof of a
303 building (20 m high); sampling at 1.5 m above the ground could promote soot-pollen

304 coagulation because, on the one hand, airborne particle concentrations can be as high
305 as 10^6 to 10^7 particles per cm^3 (Seinfeld & Pandis, 2016) and, on the other hand,
306 pollen concentrations can be higher (Charalampopoulos et al., 2021). Further
307 sampling, especially at street level, is therefore necessary to better assess the fraction
308 of PGs polluted by soot, especially as a large body of literature highlights the
309 aggravating effects on allergy of co-exposure to pollen and soot (Chen et al., 2020;
310 Nel et al., 1998; Shiraiwa et al., 2012). Unlike nasal co-deposition (Figure 5), the
311 pollen and soot (or pollen and particles) mixture resulting from atmospheric
312 coagulation may have time (up to several days) to undergo atmospheric aging.
313 Chemical reactivity at the particle-pollen contact surface cannot be excluded. Very
314 little information is available on this multiphase pollen chemistry; for example, it has
315 been shown that in the presence of moisture, allergens can diffuse from the PG to
316 soot particles deposited on its surface (Knox et al., 1997; Ormstad et al., 1998).

317 Birch pollen is never breathed alone; each inhalation introduces gaseous pollutants,
318 particles, other allergenic pollens, and other bioaerosols (viruses, bacteria, fungus
319 spores or other non-allergenic pollens) into the respiratory system. A central question
320 will be whether the level of particle deposition observed in this study on airborne
321 BPGs (0.86 particles per PG) is significant in comparison with the effects of co-
322 exposure to pollen and APM during breathing (Figure 5d). First, it should be noted
323 that the effects of these two mechanisms are cumulative; co-deposition also occurs on
324 PGs that have already been subjected to coagulation of atmospheric particles. In
325 addition, and as previously mentioned, atmospheric aging involving at least
326 biochemical reactivity and diffusion of allergens may occur after coagulation during
327 atmospheric transport of BPGs. Our study alone cannot determine the potential
328 impacts of pollen surface particle pollution on allergy. However, our atmospheric

329 observations allow to determine, for the first time without sampling artifacts, the
330 particle pollution state of the surface of inhaled pollen, which may prompt future *in*
331 *vitro* studies on the effects of the particle-pollen cocktail to use realistic particle
332 contamination of the pollen surfaces (on the order of 1%).

333 Finally, it should be mentioned that, beyond the health effects, the adhesion of
334 particles to the pollen surface could influence the reproductive capacity of pollen.
335 Some studies show a negative effect of metallic nanoparticles (Pd, Fe, ZnO) and
336 carbon particles (fullerene, graphene) on pollen reproductive capacity (Aoyagi &
337 Ugwu, 2011; Carniel et al., 2018; Dutta Gupta et al., 2019; Speranza et al., 2010, 2013;
338 Yoshihara et al., 2021). However, these studies use particularly high particle-to-
339 pollen ratios and chemical compositions that are not very representative of real
340 atmospheric particles. It was also shown that APM does not interfere with the
341 germination of *Cichorium intybus* pollen along roadsides (Jaconis et al., 2017).
342 Moreover, if the hypothesis of greater pollution of the pollen surface by particles
343 during long-distance transport is correct, it appears that the reduction of germination
344 by particle adhesion is probably insignificant because the probability of reproduction
345 between two trees located at a long distance is itself particularly low, if not zero
346 (Proctor et al., 1996).

347 **5.CONCLUSION**

348 An average pollen surface contamination of 2 ± 1 particles per BPG was obtained for
349 38% of BPGs sampled under moderate air pollution conditions (average $PM_{10} = 26.3$
350 $\mu\text{g}\cdot\text{m}^{-3}$). This value was not known in the literature because previous estimates were
351 possibly subject to sampling artifacts. Determination of this particulate
352 contamination level is important for future studies on germination or allergy as it

353 provides an estimate of a realistic dose-response effect of APM coagulated on pollen
354 surface.

355 BPGs are small (21 μm in diameter) and larger pollens could have higher APM
356 deposition rates. Gravitational settling is indeed suspected be the predominant
357 mechanism of coagulation in the atmosphere. Very little is known about pollen
358 pollution by APM on the plant, about electrostatic interactions between particles and
359 also about pollen resuspension after deposition on a surface. APM coagulation on
360 PGs could be particularly enhanced during specific atmospheric events, such as
361 thunderstorms, which can, for example, alter the electrical charges of APM and PGs,
362 increase turbulence conditions, and generate large amplitude vertical transport of
363 PGs.

364 In our current atmosphere, on a PG surface of only 1,400 μm^2 , traces of particulate
365 pollution were found on one out of three PGs. The types of particles deposited on the
366 PGs reflect the influence of human activities intensively emitting particles:
367 desertification, urban sprawl, forest fires (accentuated by climate change), intensive
368 combustion of fossil fuels and excessive industrialization.

369 **Acknowledgments**

370 MC and NV thank Université de Lille, Centre National de la Recherche Scientifique
371 (CNRS) and Institut de Recherches Pluridisciplinaires en Sciences de
372 l'Environnement (IREPSE Fed 4129) for financial support. The CaPPA project
373 (Chemical and Physical Properties of the Atmosphere) is funded by the French
374 National Research Agency (ANR) through the PIA (Programme d'Investissement
375 d'Avenir) under contract ANR-11-LABX-005-01. This work is a contribution to the
376 CPER research project CLIMIBIO. The authors thank the French Ministère de

377 l'Enseignement Supérieur et de la Recherche, the Hauts-de-France Region and the
378 European Funds for Regional Economic Development for their financial support to
379 this project.

380 **REFERENCES**

381 Aoyagi, H., & Ugwu, C. U. (2011). Fullerene Fine Particles Adhere to Pollen Grains
382 and Affect Their Autofluorescence and Germination. *Nanotechnology, Science*
383 *and Applications*, 4, 67.

384 Behrendt, H., Friedrich, K., Kainka-Stanicke, E., Darsow, U., Becker, W., &
385 Tomingas, R. (1991). Allergens and Pollutants in the Air—A Complex
386 Interaction. *New Trends in Allergy III*, 467.

387 Besancenot, J.-P., Sindt, C., & Thibaudon, M. (2019). Pollen et changement
388 climatique. Bouleau et graminées en France métropolitaine. *Revue Française*
389 *d'Allergologie*. <https://doi.org/10.1016/j.reval.2019.09.006>

390 Carniel, F. C., Gorelli, D., Flahaut, E., Fortuna, L., Casino, C. D., Cai, G., Nepi, M.,
391 Prato, M., & Tretiach, M. (2018). Graphene Oxide Impairs the Pollen
392 Performance of *Nicotiana Tabacum* and *Corylus Avellana* Suggesting
393 Potential Negative Effects on the Sexual Reproduction of Seed Plants.
394 *Environmental Science: Nano*, 5(7), 1608–1617.
395 <https://doi.org/10.1039/C8EN00052B>

396 Charalampopoulos, A., Damialis, A., Lazarina, M., Halley, J. M., & Vokou, D. (2021).
397 Spatiotemporal Assessment of Airborne Pollen in the Urban Environment: The
398 Pollenscape of Thessaloniki as a Case Study. *Atmospheric Environment*,
399 118185. <https://doi.org/10.1016/j.atmosenv.2021.118185>

400 Chen, Y., Han, L., Zhou, Y., Yang, L., & Guo, Y.-S. (2020). Artemisia Pollen Extracts
401 Exposed to Diesel Exhaust Enhance Airway Inflammation and Immunological

402 Imbalance in Asthmatic Mice Model. *International Archives of Allergy and*
403 *Immunology*, 1–11. <https://doi.org/10.1159/000505747>

404 Choël, M., Deboudt, K., & Flament, P. (2010). Development of Time-Resolved
405 Description of Aerosol Properties at the Particle Scale During an Episode of
406 Industrial Pollution Plume. *Water, Air, & Soil Pollution*, 209(1), 93–107.
407 <https://doi.org/10.1007/s11270-009-0183-9>

408 Choël, M., Ivanovsky, A., Roose, A., Hamzé, M., Blanchenet, A.-M., Deboudt, K., &
409 Visez, N. (2020). Evaluation of Hirst-Type Sampler and PM₁₀ Impactor for
410 Investigating Adhesion of Atmospheric Particles Onto Allergenic Pollen
411 Grains. *Aerobiologia*, 36, 657–668. [https://doi.org/10.1007/s10453-020-](https://doi.org/10.1007/s10453-020-09662-8)
412 [09662-8](https://doi.org/10.1007/s10453-020-09662-8)

413 Damialis, A., Gilles, S., Sofiev, M., Sofieva, V., Kolek, F., Bayr, D., Plaza, M. P., Leier-
414 Wirtz, V., Kaschuba, S., Ziska, L. H., Bielory, L., Makra, L., Trigo, M. del M.,
415 Group, C.-19/POLLEN study, & Traidl-Hoffmann, C. (2021). Higher Airborne
416 Pollen Concentrations Correlated with Increased SARS-COV-2 Infection Rates,
417 as Evidenced from 31 Countries Across the Globe. *Proceedings of the National*
418 *Academy of Sciences*, 118(12). <https://doi.org/10.1073/pnas.2019034118>

419 Darbah, J. N. T., Kubiske, M. E., Nelson, N., Oksanen, E., Vapaavuori, E., &
420 Karnosky, D. F. (2008). Effects of Decadal Exposure to Interacting Elevated
421 CO₂ and/or O₃ on Paper Birch (*Betula papyrifera*) Reproduction.
422 *Environmental Pollution*, 155(3), 446–452.
423 <https://doi.org/10.1016/j.envpol.2008.01.033>

424 Dbouk, T., & Drikakis, D. (2021). On Pollen and Airborne Virus Transmission.
425 *Physics of Fluids*, 33(6), 063313. <https://doi.org/10.1063/5.0055845>

426 Dutta Gupta, S., Saha, N., Agarwal, A., & Venkatesh, V. (2019). Silver Nanoparticles
427 (AgNPs) Induced Impairment of *in vitro* Pollen Performance of *Peltophorum*

428 *pterocarpum* (DC.) K. Heyne. *Ecotoxicology*. [https://doi.org/10.1007/s10646-](https://doi.org/10.1007/s10646-019-02140-z)
429 019-02140-z

430 Farah, J., Choël, M., de Nadaï, P., Balsamelli, J., Gosselin, S., & Visez, N. (2021).
431 Organic and Aqueous Extraction of Lipids from Birch Pollen Grains Exposed
432 to Gaseous Pollutants. *Environmental Science and Pollution Research*, 28,
433 34527–34538. <https://doi.org/10.1007/s11356-021-12940-8>

434 Frei, T. (1998). The Effects of Climate Change in Switzerland 1969–1996 on Airborne
435 Pollen Quantities from Hazel, Birch and Grass. *Grana*, 37(3), 172–179.
436 <https://doi.org/10.1080/00173139809362662>

437 García-Nieto, P. J. (2006). Study of the Evolution of Aerosol Emissions from Coal-
438 Fired Power Plants Due to Coagulation, Condensation, and Gravitational
439 Settling and Health Impact. *Journal of Environmental Management*, 79(4),
440 372–382. <https://doi.org/10.1016/j.jenvman.2005.08.006>

441 Gilles, S., Damialis, A., & Traidl-Hoffmann, C. (2021). Environmental Factors:
442 A “Missing Link” in COVID-19. *Allergo Journal International*.
443 <https://doi.org/10.1007/s40629-021-00170-w>

444 Harrison, R. G., & Carslaw, K. S. (2003). Ion-Aerosol-Cloud Processes in the Lower
445 Atmosphere. *Reviews of Geophysics*, 41(3).
446 <https://doi.org/10.1029/2002RG000114>

447 Hoebeke, L., Bruffaerts, N., Verstraeten, C., Delcloo, A., Smedt, T. D., Packeu, A.,
448 Detandt, M., & Hendrickx, M. (2017). Thirty-Four Years of Pollen Monitoring:
449 An Evaluation of the Temporal Variation of Pollen Seasons in Belgium.
450 *Aerobiologia*, 1–17. <https://doi.org/10.1007/s10453-017-9503-5>

451 Jaconis, S. Y., Culley, T. M., & Meier, A. M. (2017). Does Particulate Matter Along
452 Roadsides Interfere with Plant Reproduction? A Comparison of Effects of

453 Different Road Types on *Cichorium intybus* Pollen Deposition and
454 Germination. *Environmental Pollution*, 222, 261–266.

455 Khaiwal, R., Goyal, A., & Mor, S. (2021). Does Airborne Pollen Influence COVID-19
456 Outbreak? *Sustainable Cities and Society*, 102887.
457 <https://doi.org/10.1016/j.scs.2021.102887>

458 Knox, R. B., Suphioglu, C., Taylor, P., Desai, R., Watson, H. C., Peng, J. L., & Bursill,
459 L. A. (1997). Major Grass Pollen Allergen Lol p 1 Binds to Diesel Exhaust
460 Particles: Implications for Asthma and Air Pollution. *Clinical & Experimental*
461 *Allergy*, 27(3), 246–251. <https://doi.org/10.1111/j.1365-2222.1997.tb00702.x>

462 Lavaud, F., Fore, M., Fontaine, J. F., Pérotin, J. M., & de Blay, F. (2013). Allergie au
463 pollen de bouleau. *Revue Des Maladies Respiratoires*, 31(2), 150–161.
464 <https://doi.org/10.1016/j.rmr.2013.08.006>

465 Levetin, E. (2004). Methods for Aeroallergen Sampling. *Current Allergy and Asthma*
466 *Reports*, 4(5), 376–383. <https://doi.org/10.1007/s11882-004-0088-z>

467 Mullins, J., & Emberlin, J. (1997). Sampling Pollens. *Journal of Aerosol Science*,
468 28(3), 365–370. [https://doi.org/10.1016/S0021-8502\(96\)00439-9](https://doi.org/10.1016/S0021-8502(96)00439-9)

469 Nel, A. E., Diaz-Sanchez, D., Ng, D., Hiura, T., & Saxon, A. (1998). Enhancement of
470 Allergic Inflammation by the Interaction Between Diesel Exhaust Particles and
471 the Immune System. *Journal of Allergy and Clinical Immunology*, 102(4),
472 539–554. [https://doi.org/10.1016/S0091-6749\(98\)70269-6](https://doi.org/10.1016/S0091-6749(98)70269-6)

473 Okuyama, Y., Matsumoto, K., Okochi, H., & Igawa, M. (2007). Adsorption of Air
474 Pollutants on the Grain Surface of Japanese Cedar Pollen. *Atmospheric*
475 *Environment*, 41(2), 253–260.

476 Ormstad, H., Johansen, B., & Gaarder, P. (1998). Airborne House Dust Particles and
477 Diesel Exhaust Particles as Allergen Carriers. *Clinical and Experimental*
478 *Allergy*, 28(6), 702–708.

479 Pereira, S., Fernández-González, M., Guedes, A., Abreu, I., & Ribeiro, H. (2021). The
480 Strong and the Stronger: The Effects of Increasing Ozone and Nitrogen
481 Dioxide Concentrations in Pollen of Different Forest Species. *Forests*, 12(1),
482 88. <https://doi.org/10.3390/f12010088>

483 Proctor, M., Yeo, P., & Lack, A. (1996). *The Natural History of Pollination* (Updated,
484 Subsequent). Timber Press.

485 Ribeiro, H., Guimarães, F., Duque, L., Noronha, F., & Abreu, I. (2015).
486 Characterisation of Particulate Matter on Airborne Pollen Grains.
487 *Environmental Pollution*, 206, 7–16.
488 <https://doi.org/10.1016/j.envpol.2015.06.015>

489 Robichaud, A. (2021). A Case Study of Birch Pollen and the Synergy with
490 Environmental Factors: Relation to Asthma in Montreal, Canada. *Atmosphere*,
491 12(6), 789. <https://doi.org/10.3390/atmos12060789>

492 Roos, R. A., & Dutertre-Laduree, D. (1990). Atmospheric Charged Aerosol and
493 Electric Field Observations in Western France. *Journal of Aerosol Science*, 21,
494 S283–S286. [https://doi.org/10.1016/0021-8502\(90\)90239-T](https://doi.org/10.1016/0021-8502(90)90239-T)

495 Ruggiero, F., & Bedini, G. (2018). Systematic and Morphologic Survey of Orbicules in
496 Allergenic Angiosperms. *Aerobiologia*, 34, 405–422.

497 Ruggiero, F., & Bedini, G. (2020). Phylogenetic and Morphologic Survey of Orbicules
498 in Angiosperms. *TAXON*, 69(3), 543–566. <https://doi.org/10.1002/tax.12281>

499 Schiavoni, G., D'Amato, G., & Afferni, C. (2017). The Dangerous Liaison Between
500 Pollens and Pollution in Respiratory Allergy. *Annals of Allergy, Asthma &*
501 *Immunology*, 118(3), 269–275.

502 Seinfeld, J. H., & Pandis, S. N. (2016). *Atmospheric Chemistry and Physics: From*
503 *Air Pollution to Climate Change*. John Wiley & Sons.

504 Sénéchal, H., Visez, N., Charpin, D., Shahali, Y., Peltre, G., Bioley, J.-P., Lhuissier, F.,
505 Couderc, R., Yamada, O., Malrat-Domenge, A., Pham Thi, N., Poncet, P., &
506 Sutra, J.-P. (2015). A Review of the Effects of Major Atmospheric Pollutants on
507 Pollen Grains, Pollen Content and Allergenicity. *The Scientific World Journal*,
508 2015, ID 940243. <https://doi.org/10.1155/2015/940243>

509 Shao, S., Zhou, D., He, R., Li, J., Zou, S., Mallery, K., Kumar, S., Yang, S., & Hong, J.
510 (2021). Risk assessment of airborne transmission of COVID-19 by
511 asymptomatic individuals under different practical settings. *Journal of*
512 *Aerosol Science*, 151, 105661. <https://doi.org/10.1016/j.jaerosci.2020.105661>

513 Shiraiwa, M., Selzle, K., & Pöschl, U. (2012). Hazardous Components and Health
514 Effects of Atmospheric Aerosol Particles: Reactive Oxygen Species, Soot,
515 Polycyclic Aromatic Compounds and Allergenic Proteins. *Free Radical*
516 *Research*, 46(8), 927–939.

517 Sofiev, M., Siljamo, P., Ranta, H., & Rantio-Lehtimäki, A. (2006). Towards Numerical
518 Forecasting of Long-Range Air Transport of Birch Pollen: Theoretical
519 Considerations and a Feasibility Study. *International Journal of*
520 *Biometeorology*, 50(6), 392–402. [https://doi.org/10.1007/s00484-006-](https://doi.org/10.1007/s00484-006-0027-x)
521 [0027-x](https://doi.org/10.1007/s00484-006-0027-x)

522 Speranza, A., Crinelli, R., Scoccianti, V., Taddei, A. R., Iacobucci, M., Bhattacharya,
523 P., & Ke, P. C. (2013). *In-Vitro* Toxicity of Silver Nanoparticles to Kiwifruit
524 Pollen Exhibits Peculiar Traits Beyond the Cause of Silver Ion Release.
525 *Environmental Pollution*, 179, 258–267.
526 <https://doi.org/10.1016/j.envpol.2013.04.021>

527 Speranza, A., Leopold, K., Maier, M., Taddei, A. R., & Scoccianti, V. (2010). Pd-
528 Nanoparticles Cause Increased Toxicity to Kiwifruit Pollen Compared to
529 Soluble Pd (ii). *Environmental Pollution*, 158(3), 873–882.

530 Visez, N., Ivanovsky, A., Roose, A., Gosselin, S., Sénéchal, H., Poncet, P., & Choël, M.
531 (2020). Atmospheric Particulate Matter Adhesion onto Pollen: A Review.
532 *Aerobiologia*, 36(1), 49–62. <https://doi.org/10.1007/s10453-019-09616-9>

533 Wittmaack, K., Wehnes, H., Heinzmann, U., & Agerer, R. (2005). An Overview on
534 Bioaerosols Viewed by Scanning Electron Microscopy. *Science of The Total*
535 *Environment*, 346(1), 244–255.
536 <https://doi.org/10.1016/j.scitotenv.2004.11.009>

537 Xie, X., Li, Y., Sun, H., & Liu, L. (2009). Exhaled Droplets Due to Talking and
538 Coughing. *Journal of The Royal Society Interface*, 6(suppl_6), S703–S714.
539 <https://doi.org/10.1098/rsif.2009.0388.focus>

540 Yoshihara, S., Hirata, S., Yamamoto, K., Nakajima, Y., Kurahashi, K., & Tokumoto, H.
541 (2021). ZnO Nanoparticles Effect on Pollen Grain Germination and Pollen
542 Tube Elongation. *Plant Cell, Tissue and Organ Culture (PCTOC)*.
543 <https://doi.org/10.1007/s11240-021-02017-2>

544 Zhu, C., Farah, J., Choël, M., Gosselin, S., Baroudi, M., Petitprez, D., & Visez, N.
545 (2018). Uptake of Ozone and Modification of Lipids in *Betula Pendula* Pollen.
546 *Environmental Pollution*, 242, 880–886.
547 <https://doi.org/10.1016/j.envpol.2018.07.025>

548 Ziska, L. H., Makra, L., Harry, S. K., Bruffaerts, N., Hendrickx, M., Coates, F., Saarto,
549 A., Thibaudon, M., Oliver, G., Damialis, A., Charalampopoulos, A., Vokou, D.,
550 Heidmarsson, S., Gudjohansen, E., Bonini, M., Oh, J.-W., Sullivan, K., Ford, L.,
551 Brooks, G. D., ... Crimmins, A. R. (2019). Temperature-Related Changes in
552 Airborne Allergenic Pollen Abundance and Seasonality Across the Northern
553 Hemisphere: A Retrospective Data Analysis. *The Lancet Planetary Health*,
554 3(3), e124–e131. [https://doi.org/10.1016/S2542-5196\(19\)30015-4](https://doi.org/10.1016/S2542-5196(19)30015-4)

555

